Design of Tapered Slot Antenna Divided Into Some Parts

Kuniaki Suto, Akinori Matsui
Saitama Institute of Technology
Graduate School Department of Electronic Engineering
Fukaya-shi Saitama, Japan

***Abstract*—This paper proposes a design method for a tapered slot antenna divided into parts. Previous reports have discussed the matching characteristics obtained by the S-parameter method related to the measurement of the input impedance. In these reports, the measured and simulated input impedances were shown to differ in the high frequency region. This article shows that better agreement can be achieved by the appropriate compensation of the feed reference. Moreover, a design parameter for the taper is introduced when a high gain and low sidelobe level are obtained.**

Keywords*—*Tapered slot antenna; S-parameter method; Input impedance; Radiation characteristics

I. INTRODUCTION

A tapered slot antenna (TSA) is an antenna that radiates unidirectionally over a wide frequency range. TSAs have been investigated for their application in ground-penetrating radar (GPR) and base station antennas, which communicate across multiple frequencies, in addition to other applications [1][2]. However, because TSAs are a type of traveling wave antenna, the values of many parameters must be selected, which complicates the design.

Our goal is to design TSA using a simple technique. This paper presents a design method that divides the TSA into a radiator and a balun, which is a device that converts between balanced and unbalanced signals, and discusses how to select the parameters of the parts such that the TSA shows good performance [3]. The matching characteristics obtained by the S-parameter method [4] related to the measurement of the input impedance Z_{in} were discussed in a previous study [3]. An earlier study investigated radiation only from the radiator, excluding that from the antenna feed [5]; in this study, the measurement was performed using a 3 dB 180° hybrid coupler (HYB). The issue remaining from a previous report [4] is that the difference between the simulation and measurement results increases when frequencies exceed 8 GHz, although the antenna is designed to operate within the range of 3–11 GHz.

In this paper, good agreement between the simulation and measurement results is demonstrated by tuning the electrical delay at the input (feed) port. Therefore, the input impedance Z_{in} can be estimated. Furthermore, the charts in this paper are more detailed than the descriptions of the radiator design given in previous reports. The minimum number of frequency points is discussed with regard to the radiation characteristics because numerous simulation points are needed for the wide-frequency range antenna, which requires a long simulation time. An investigation of three points (3, 7, and 11 GHz) within the designed frequency (3–11 GHz) reveals that the sidelobe level (SLL) can be estimated.

II. CONFIGURATION

Figure 1 illustrates the configuration of the TSA. The TSA is fabricated on a dielectric substrate (Teflon glass fiber substrate with a dielectric constant ε_r of 2.6 and a thickness h of 0.6 mm). The radiator is of length L and width W and has a linear taper. The slot line (SL) is fabricated on the same side as the radiator, and the microstrip line (MSL) is fabricated on the opposite side. The MSL and the SL constitute an electromagnetically coupled transition (balun). The radiator and the balun are connected by a coplanar strip line (CPS). The characteristic impedances of the SL and CPS are set at the same value to prevent mismatching (125 Ω). Electromagnetic simulator WIPL-D is used in the simulations.

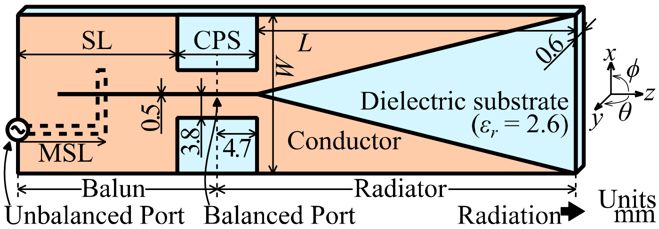

Fig. 1. Configuration of TSA.

III. Input Impedance

To make the TSA radiate starting at a minimum frequency of 3 GHz, the radiator dimensions are set to $L = \lambda = 100$ mm and $W = \lambda/2 = 50$ mm. A measurement is performed using the S-parameter method to obtain Z_{in}. The radiator of a balanced one-port circuit is regarded as equivalent to an unbalanced two-port circuit in Fig. 2. Z_{in} is estimated from [4]

$$Z_{in} = 2Z_{na}\frac{1+S_{11}-S_{21}}{1-S_{11}+S_{21}}, \tag{1}$$

where Z_{na} is the impedance of the measurement system (50 Ω). Conversely, a balanced current flows into the radiator in the simulation. The feeding structure is shown in Fig. 2 (b). The tops of two small metal trapezoids facing each other are connected by the wire through which the current is generated, and the bottoms are connected to the edge of the CPS. The electrical length reference L_e in the simulation is tuned to ensure agreement with the measurement. L_e is set to 1.93 mm, which means that 1.9 mm is added to the length from the edge to the center of the CPS and 0.03 mm to the height of the trapezoid.

Figure 3 illustrates the resistance component R and the reactance component X of Z_{in}. The differences between the maximum measured and simulated R and X values are compared for two values of L_e; these R and X values are given in Table 1. The differences between the measured and simulated values are –25.2 Ω for R and –34 Ω for X when the frequency, $f < 8$ GHz and $L_e = 0$ mm (points A and B). These values indicate good agreement between the measurement and the simulation. However, the differences at points C and D increase when $f > 8$ GHz. When $L_e = 1.93$ mm, the differences at points A and B become relatively large: –38.0 Ω for R and –39.7 Ω for X. Conversely, the difference decreases with increasing L_e at points C and D. The values change from –77.7 to –13.3 Ω for R and from –64.8 Ω to –37.4 Ω for X. The simulation achieves good agreement with the measurement in the region from 3 to 11 GHz when $L_e = 1.93$ mm. Appropriately tuning the electrical reference position demonstrates that the simulation is a valuable technique for this type of TSA and is effective in the design of the radiator.

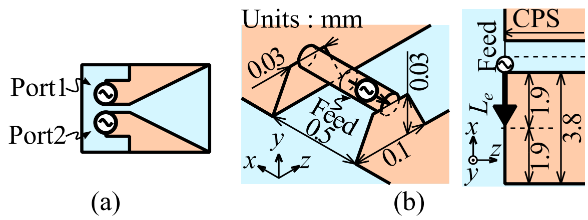

Fig. 2. Feed structure. (a) Measurment (S-parameter method). (b) Simulation (balanced current feed).

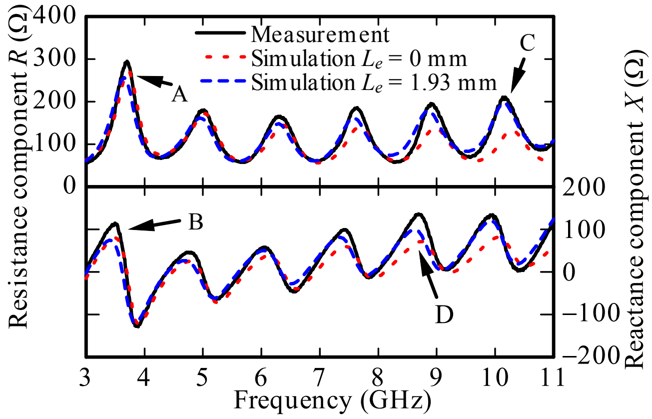

Fig. 3. Resistance R and reactance X components of input impedance Z_{in} (L = 100 mm, W = 50 mm).

TABLE I. Measured and Simulated Resistance and Reactance Components of Input Impedance

		Input impedance			
		Under 8 GHz		Over 8 GHz	
		R Point A	X Point B	R Point C	X Point D
Measurement		294.3 Ω	113.8 Ω	210.4 Ω	136.0 Ω
Simulation	L_e = 0 mm	269.2 Ω	79.8 Ω	132.7 Ω	71.2 Ω
	L_e = 1.93 mm	256.4 Ω	74.0 Ω	197.1 Ω	98.7 Ω

IV. Design for Radiation

Radiation at 3, 7, and 11 GHz within the frequency band of 3–11 GHz is simulated to simplify the discussion. Because L and W are presumed to be significant parameters, we investigate the effect of L and W on the radiation. Color maps of the simulation results, in which the length L and width W are varied from 20 to 200 mm and 20 to 100 mm, respectively, in steps of 20 mm, are shown in Fig. 4. The maximum values of the results of the simulations at 3, 7, and 11 GHz are illustrated as color maps. When the dimensions are related as approximately $W = L/2 + 20$, the highest boresight gain is obtained. This line is represented by a broken line in each part of the figure. Figure 4 (b), which shows the half power bandwidth (HPW) of the H-plane, indicates that the HPW reaches approximately 135° during high-gain performance for dimensions in the range of 60 mm < L < 120 mm and 50 mm < W < 80 mm. Figure 4 (c) and (d), which shows the SLL in the boresight of the E- and H-planes, demonstrates that the SLL is suppressed and remains under approximately –6 dB.

From the above discussion, we tested the TSA with L = 120 mm and W = 80 mm, as described in the following, because a high gain and low SLL are expected. The radiation patterns of the measurement and the simulation of the test TSA are displayed in Fig. 5 as color maps. The x-axis represents the frequency, and the y-axis represents the angle. The color illustrates the ratio of the radiated power. A 3 dB 180° HYB was used to measure the radiation pattern, as in a previous report [5]. Therefore, the radiation from the radiator is observed without the effect of the feed system. The simulation is in good agreement with the measurement in both planes. The area near 0° shows the peak radiation. All patterns are symmetric about $\theta = 0°$ and $\phi = 0°$. Moreover, the HPWs of the experiments agree with the simulation results. We confirm that the simulation is an effective method of accurately estimating the radiation from the radiator. Further, the efficiency of the gain to the directivity in the bore sight is approximately achieved more than 80% up to 8GHz, 70% from 8GHz to 7GHz and 60% more than 10GHz. Figure 6 shows the photo of the radiation pattern measurement of the radiator with HYB.

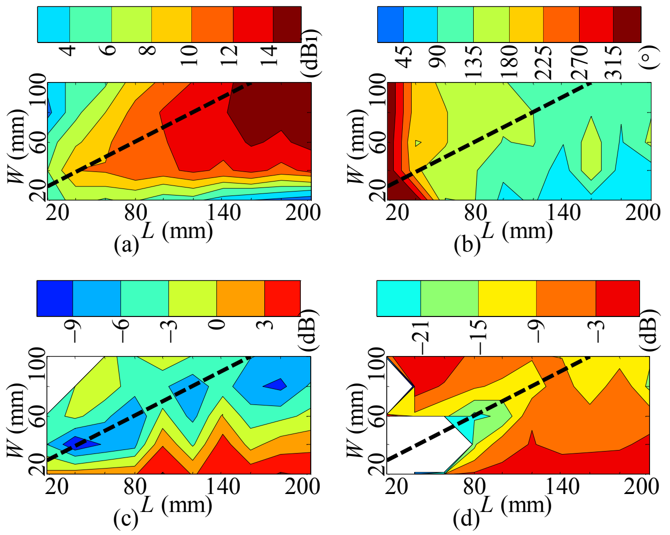

Fig. 4. Radiation pattern. (a) Gain (dBi). (b) H-plane HPW (°). (c) E-plane SLL (dB). (d) H-plane SLL (dB). (The dashed line indicates the dimensions that yield the highest gain.)

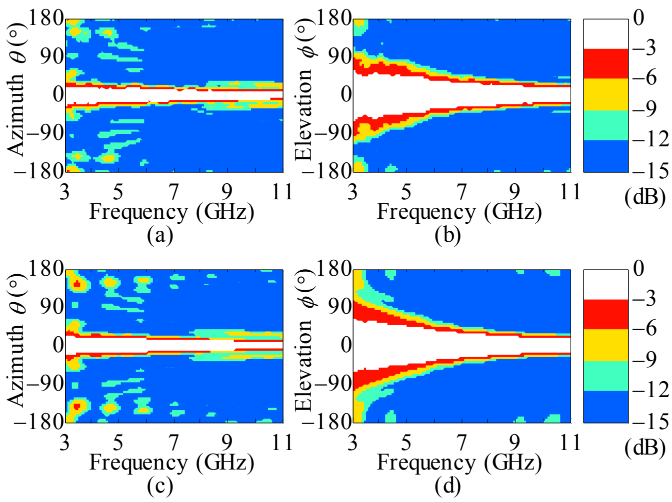

Fig. 5. Variation in radiation with frequency. (L = 120 mm, W = 80 mm) (a) E- and (b) H-planes for measurement results. (c) E- and (d) H-planes for simulation results.

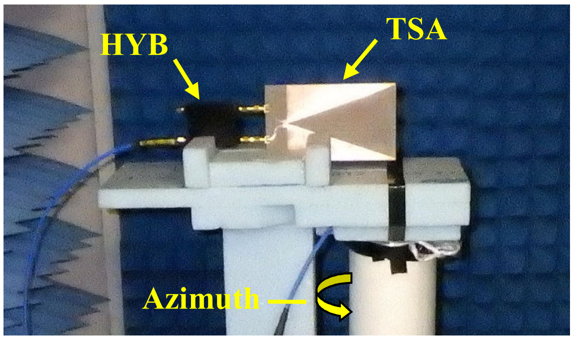

Fig. 6. Radiation pattern measurement of the TSA

V. Conclusion

In this paper, we proposed a TSA design technique that divides the antenna into the feed structure and the radiator. The input impedance, which is tuned to the feed reference in the simulation, and the radiation from the radiator excluding the feed system, which can be estimated using the simulation, were obtained and tested. The Z_{in} results of the compensated simulation were shown to be in good agreement with the measurement results within the frequency range of 3–11 GHz. Moreover, regarding the radiation, the SLL of the radiation was able to be specified within the frequency range in simulations of the lowest, middle, and highest frequencies.

We consider the remaining problems to be that the feeding structure in the simulation should be discussed in more detail and the radiator design should consider other parameters, such as the front–back ratio, rather than only the SLL. The design or optimization of the balun also remains as a future challenge. We expect that this will be accomplished by expanding the S-parameter method.

References

[1] Akira Hirose, Ayato Ejiri and Kunio Kitahara, "Generation of landmine concept among multiple SOMs utilizing mutual information," 2010 IEICE Technical Report, vol. 109, no. 461, pp. 249–254, Mar. 2010.

[2] Kazuya Itoh, Keisuke Konno, QiangChen and Shingo Inoue, "Design of Compact Multiband Antenna for Triple-Band Cellular Base Stations," IEEE Antennas and Wireless Propagation Letters, vol. 14, pp. 64–67, Jan. 2015.

[3] Kuniaki Suto and Akinori Matsui, "Input Impedance of Tapered Slot Antenna by S-Parameter Method," IEICE Transactions on Communications, vol. J98-B, no. 1, pp. 98–102, Jan. 2015.

[4] Rene Meys and Frederic Janssens, "Measuring the Impedance of Balanced Antennas by an S-Parameter Method," IEEE Antennas Propagation Magazine, vol. 40, no. 6, pp. 62–65, Dec. 1998.

[5] Kuniaki Suto and Akinori Matsui, "Radiation Characteristic of Tapered Slot Antenna with 3dB 180° Hybrid Coupler," 2014ISAP, TH4A-05, Dec. 2014.